

Supporting Information

© Wiley-VCH 2014

69451 Weinheim, Germany

**The Strongest Brønsted Acid: Protonation of Alkanes by $\text{H}(\text{CHB}_{11}\text{F}_{11})$
at Room Temperature****

*Matthew Nava, Irina V. Stoyanova, Steven Cummings, Evgenii S. Stoyanov, and
Christopher A. Reed**

anie_201308586_sm_miscellaneous_information.pdf

Contents:

Figs. S1-S4: IR, ^{19}F , ^{11}B NMR and mass spectra of $\text{Cs}(\text{CHB}_{11}\text{F}_{11})$

Figs. S5-S6: IR and ^1H NMR spectra of $\text{AgCHB}_{11}\text{F}_{11} \cdot 2\text{C}_6\text{H}_6$

Figs. S7-S8: IR and ^1H NMR spectra of $[(\text{C}_6\text{H}_5)_3\text{C}][\text{CHB}_{11}\text{F}_{11}]$

Fig. S9: IR spectrum of $[(\text{Et}_3\text{Si})_2\text{H}][\text{CHB}_{11}\text{F}_{11}]$

Fig. S10: IR spectrum of protio and deuterio $\text{H}(\text{CHB}_{11}\text{F}_{11})$

Fig. S11: IR spectrum of $[\text{H}_3\text{O}^+][\text{CHB}_{11}\text{F}_{11}]$

Fig. S12: IR spectrum of $[\text{C}_6\text{H}_7][\text{CHB}_{11}\text{F}_{11}]$ compared to $[\text{C}_6\text{H}_7][\text{CHB}_{11}\text{Cl}_{11}]$

Fig. S13: Gas Chromatographic trace showing the detection of H_2

Fig. S14: IR spectrum of carbocation(s) from protonation of *n*-hexane

Fig. S15-S17: IR spectrum of *t*-butyl cation from protonation of *n*-butane, compared to $[t\text{-Bu}^+][\text{CHB}_{11}\text{Cl}_{11}^-]$.

Fig. S18-S20: Gc and mass spectral data showing the production of hexene from C_6 carbocation salt and NaH in SO_2 .

Fig. S21: Gc of alkanes produced by reaction of ground $\text{NaH}_{(s)}$ with C_6 carbocation salts.

Fig. S22: Gc of *iso*-butane produced by reaction of ground $\text{NaH}_{(s)}$ with $t\text{-Bu}^+ [\text{CHB}_{11}\text{F}_{11}^-]$.

(17 pages)

Fig. S1. ATR-IR spectrum of Cs(CHB₁₁F₁₁):

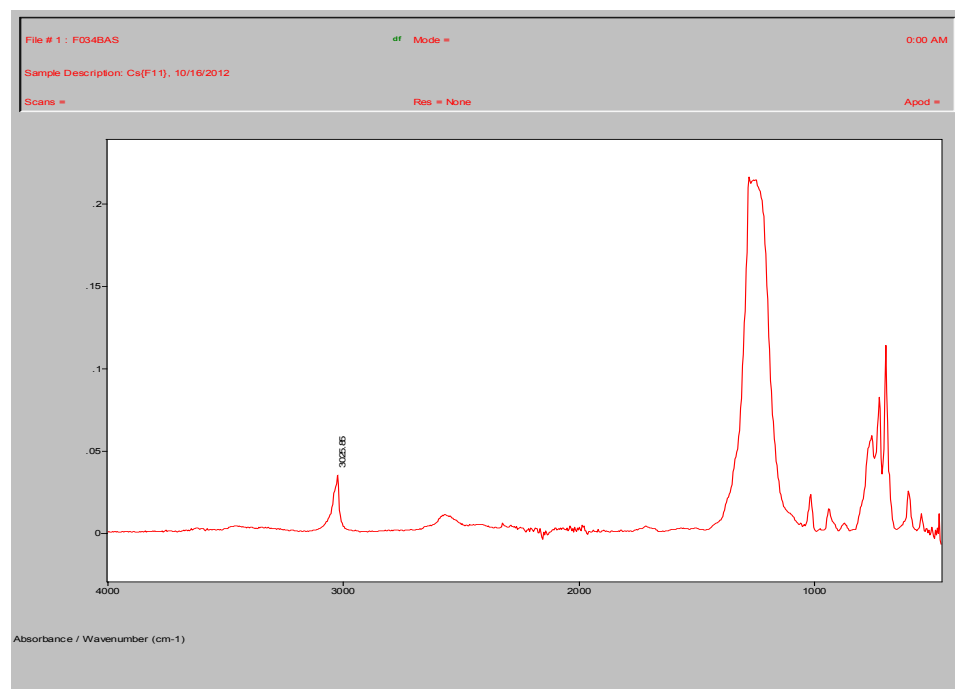


Fig. S2. ¹⁹F NMR Cs(CHB₁₁F₁₁) in acetone-*d*₆:

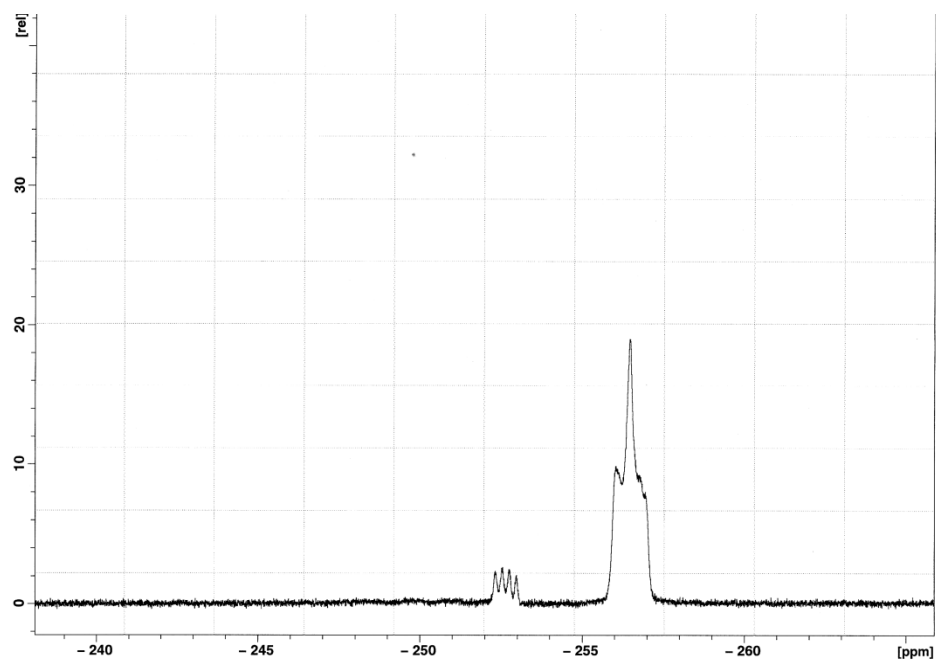


Fig. S3. ^{11}B NMR $\text{Cs}(\text{CHB}_{11}\text{F}_{11})$ in acetone- d_6 :

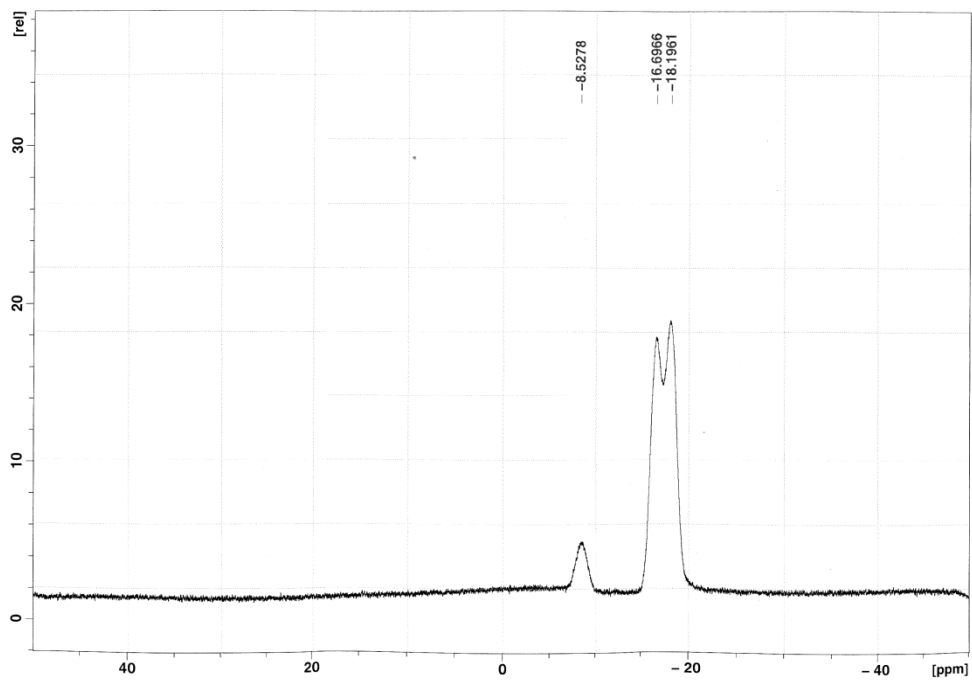


Fig. S4. Negative ion electrospray ionization mass spectrum of $\text{Cs}(\text{CHB}_{11}\text{F}_{11})$:

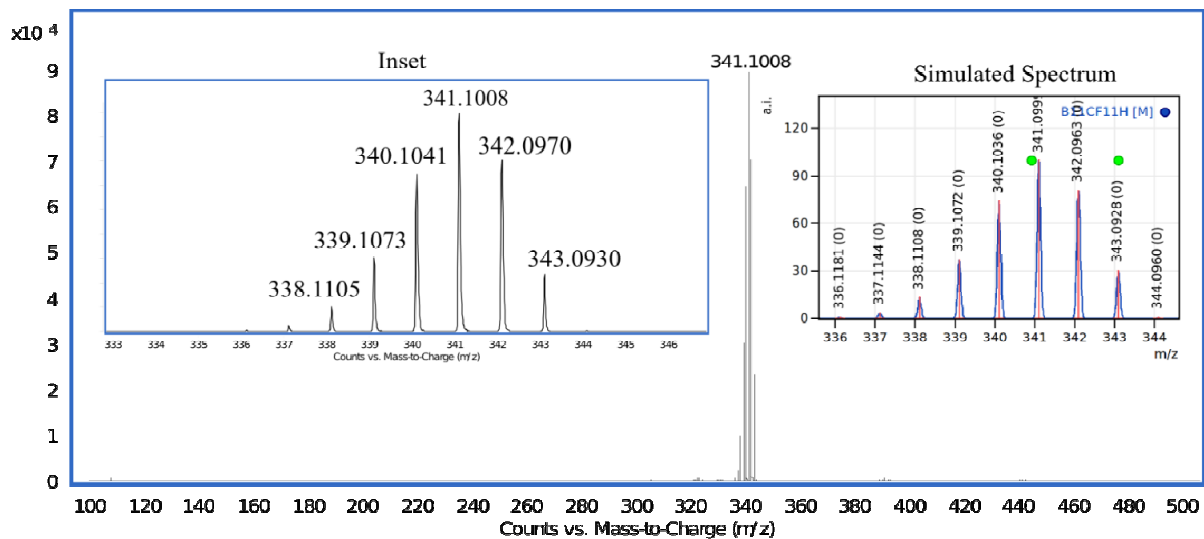


Fig. S5. ATR IR spectrum of $\text{Ag}(\text{CHB}_{11}\text{F}_{11}) \cdot 2\text{C}_6\text{H}_6$:

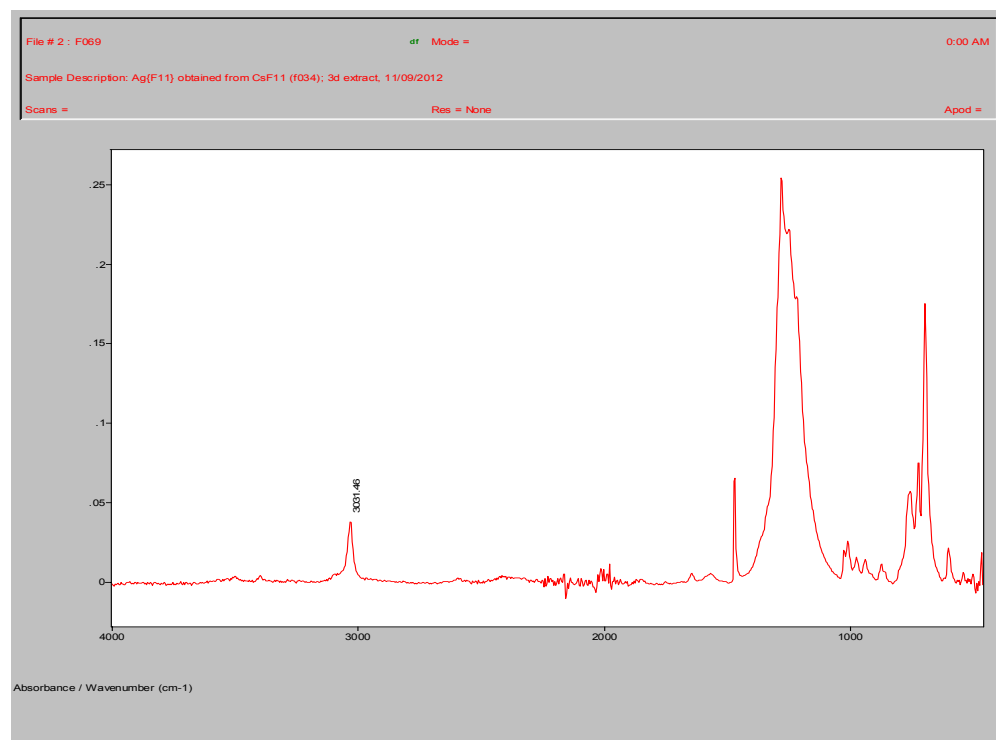


Fig. S6. ^1H NMR spectrum of $\text{Ag}(\text{CHB}_{11}\text{F}_{11}) \cdot 2\text{C}_6\text{H}_6$:

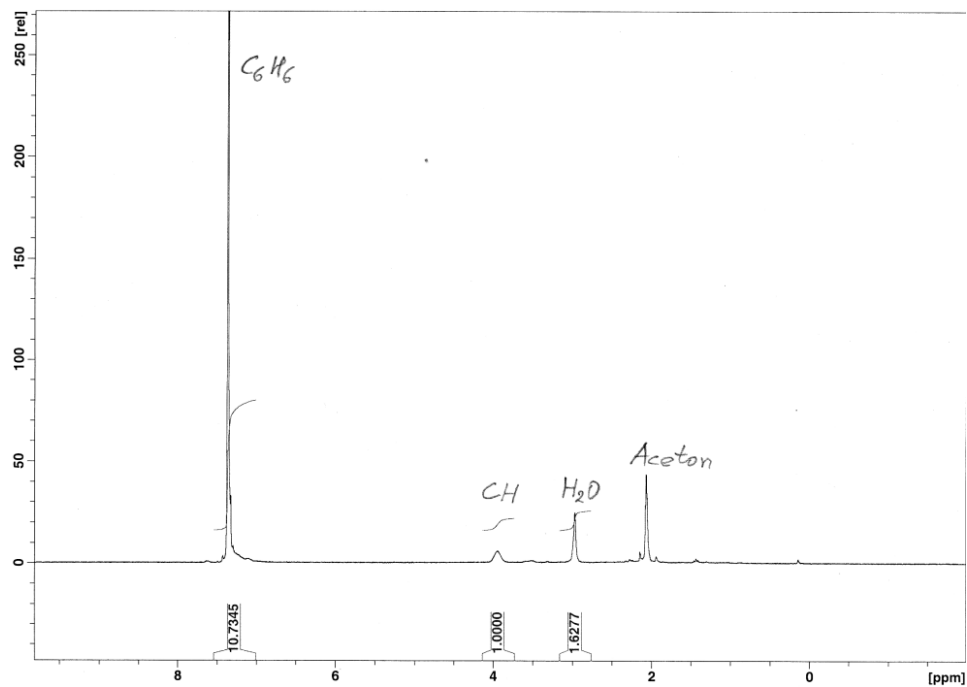


Fig. S7. ATR IR spectrum of $[(C_6H_5)_3C][CHB_{11}F_{11}]$:

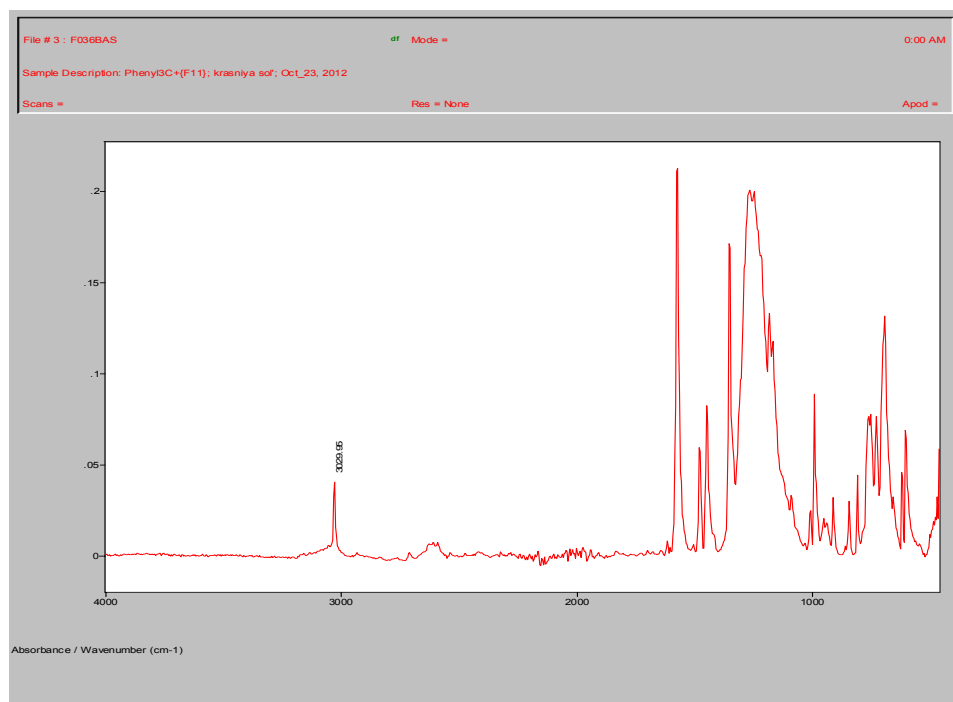


Fig. S8. ¹H NMR $[(C_6H_5)_3C][CHB_{11}F_{11}]$ in CD₂Cl₂.

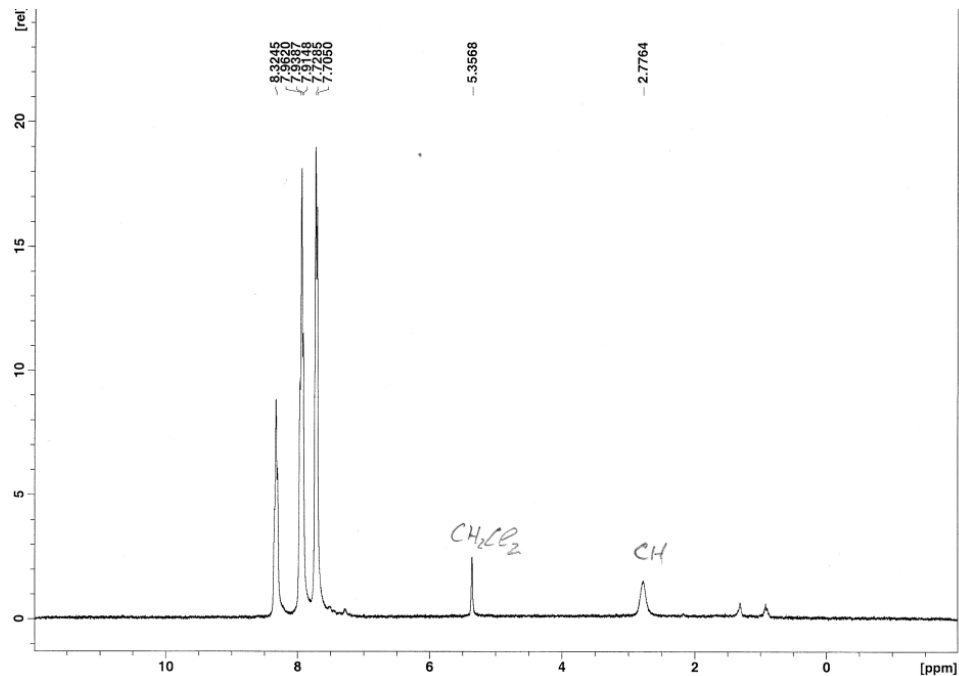


Fig. S9. ATR IR spectrum of $[(Et_3Si)_2H][(CHB_{11}F_{11})]$. Note the diagnostic $\nu SiHSi$ band at 1873 cm^{-1} .^[25]

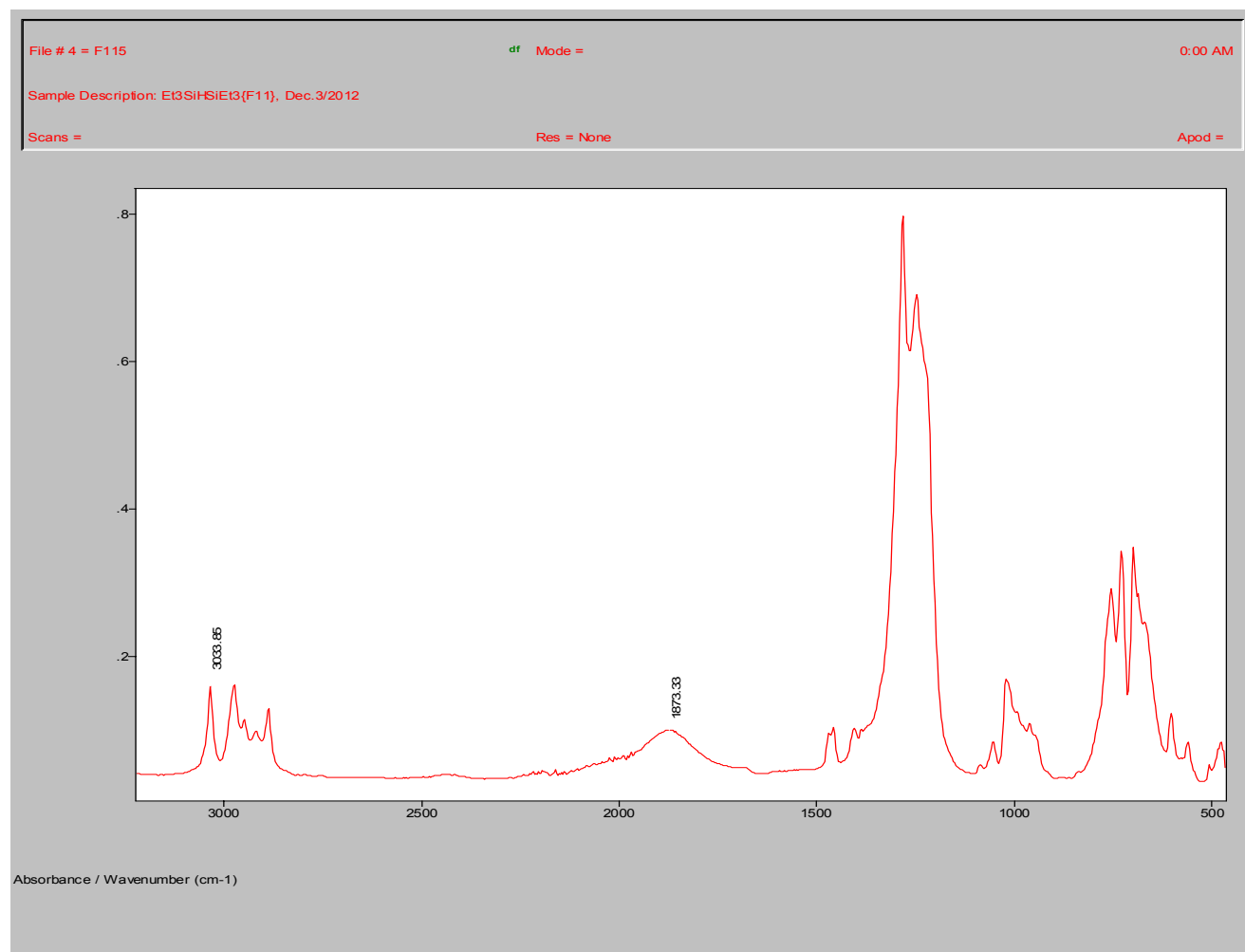


Fig. S10. Comparison of IR spectra of protio (blue) and deuterio (red) $\text{H}(\text{CHB}_{11}\text{F}_{11})$ with assignments indicated below. Unaffected peaks (black font in assignments given below) are νCH of the anion at 3029 cm^{-1} , νBB at ca. 1200 cm^{-1} (which happens to coincide with νFDF) and four relatively sharp νBF bands in the 700 cm^{-1} region. Complexity in the region below 1000 cm^{-1} indicates that δFHF and/or δFDF are broad and either anharmonic or subject to distortions from resonance effects leading to transparent windows (Evans holes), an effect commonly observed in strongly H-bonded systems. See discussion in ref. 14, p13872.

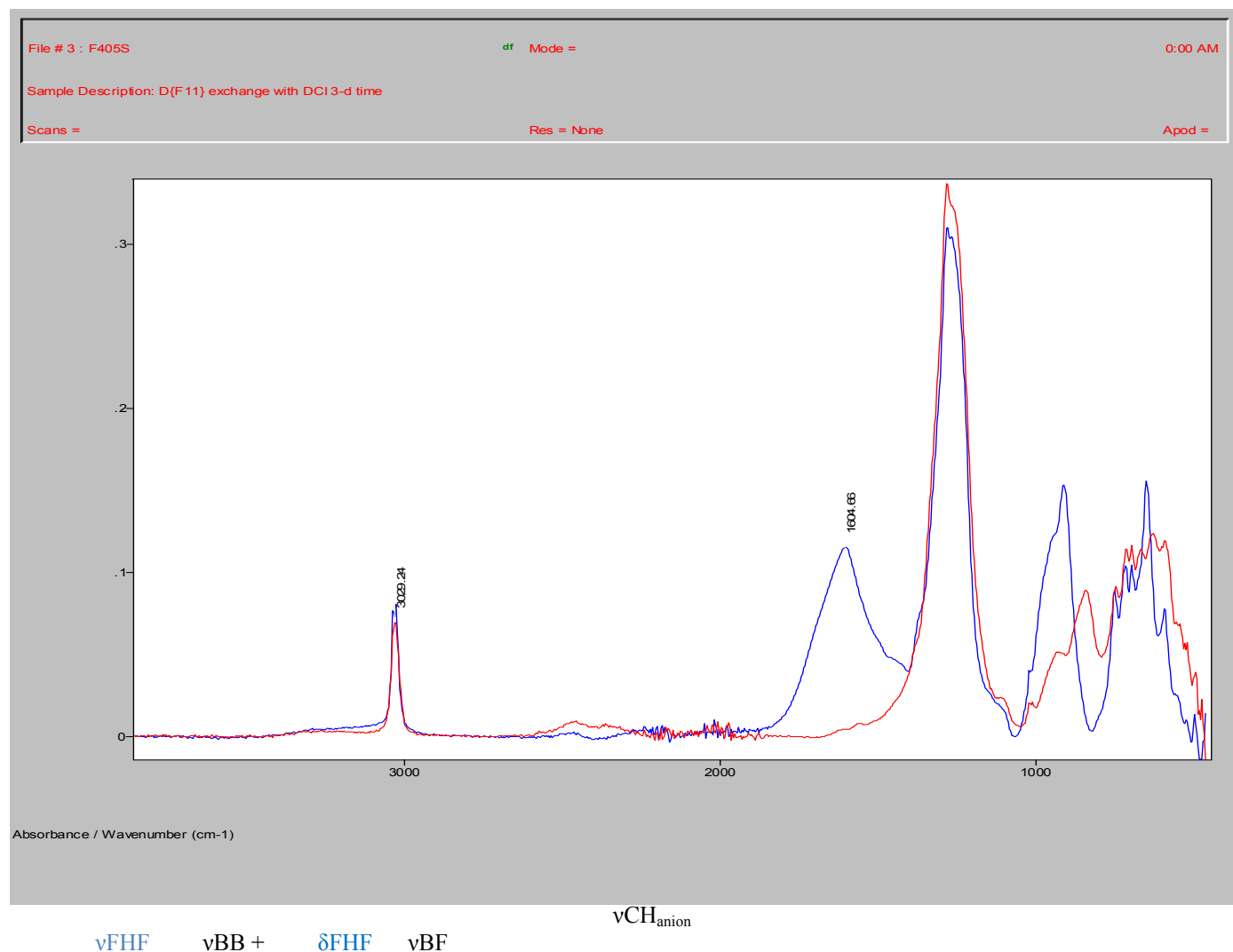


Fig. S11. IR spectrum of $[\text{H}_3\text{O}][\text{CHB}_{11}\text{F}_{11}]$ from minimal exposure of $\text{H}(\text{CHB}_{11}\text{F}_{11})$ to moist air:

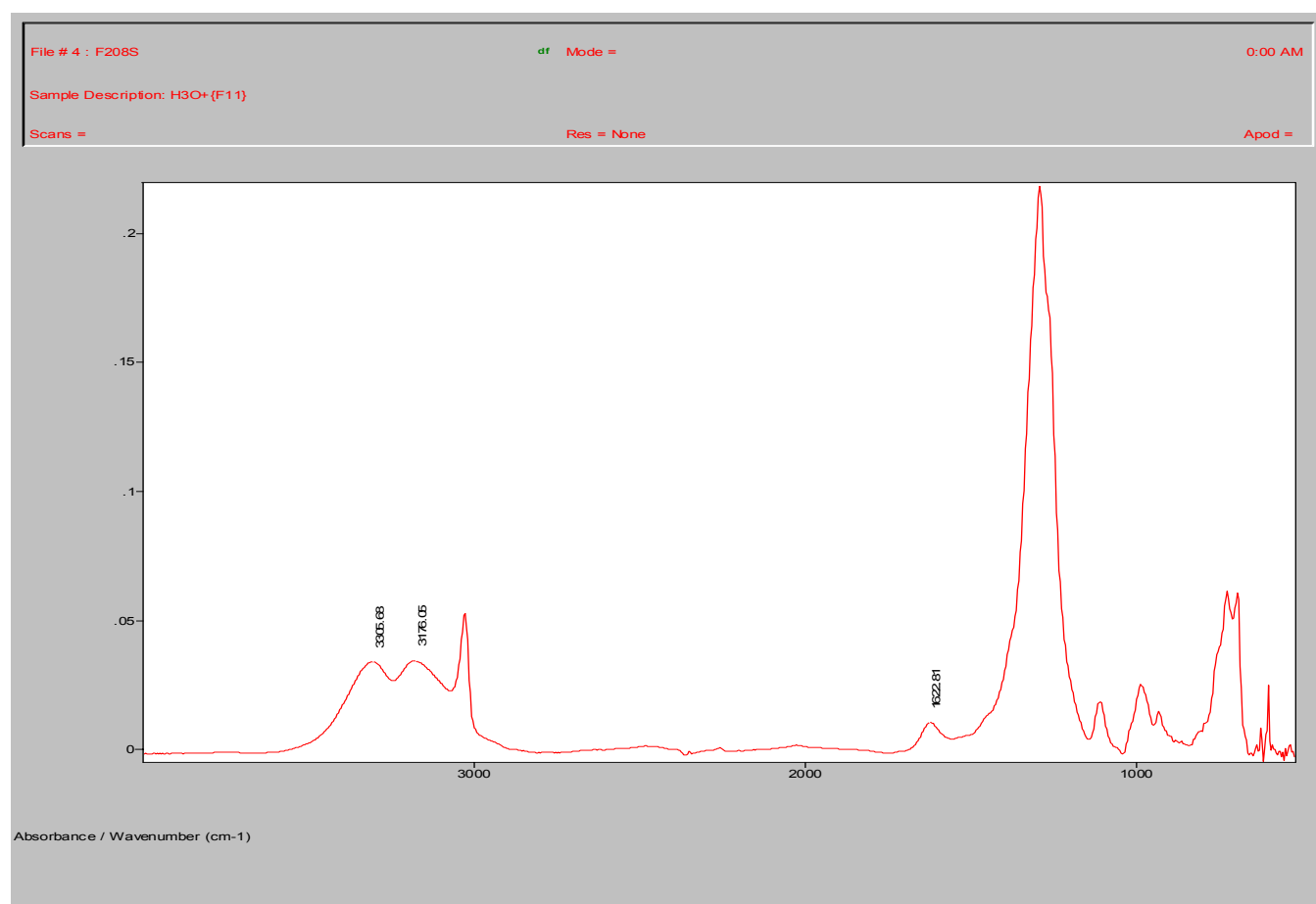


Fig. S12. IR spectra of the benzenium ion salt $[\text{C}_6\text{H}_7][\text{CHB}_{11}\text{F}_{11}]$ from contact of $\text{H}(\text{CHB}_{11}\text{F}_{11})_{(s)}$ with dry benzene (red) compared with that of known $[\text{C}_6\text{H}_7][\text{CHB}_{11}\text{Cl}_{11}]$ (blue). The ring $\nu\text{C-C}$ bands near 1500 cm^{-1} coincide but the νCH bands vary with anion because of H-bonding. The νCH bands are assigned as follows: sp^2 aromatic ca. 3100 cm^{-1} , carborane anion 3029 cm^{-1} and sp^3 $2700\text{-}2820\text{ cm}^{-1}$.

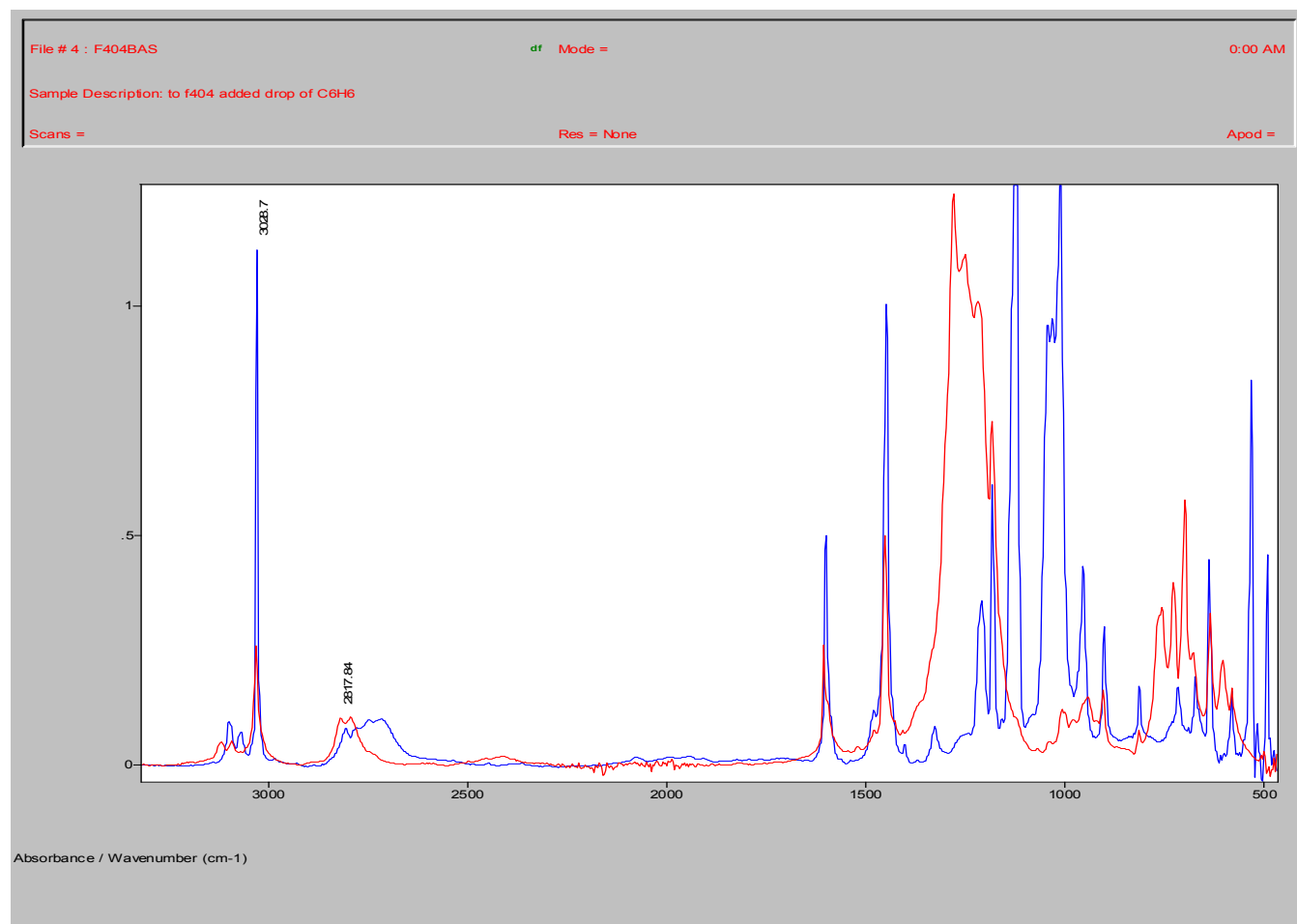


Fig. S13. Gas Chromatographic trace for detection of H₂ (1.7 min) from the reaction of H(CHB₁₁F₁₁) with hexane under N₂ (3.7 min). About 50 mg of H(CHB₁₁F₁₁) was placed in a Schlenk tube under an N₂ atmosphere inside a glove box and 0.5 ml of *n*-hexane was added. After 8 h, when ca. 75% of acid was converted to carbocation salt(s), the gaseous phase was analyzed. Prior to this analysis, the gc was calibrated with a gas sample known to contain dihydrogen in dinitrogen.

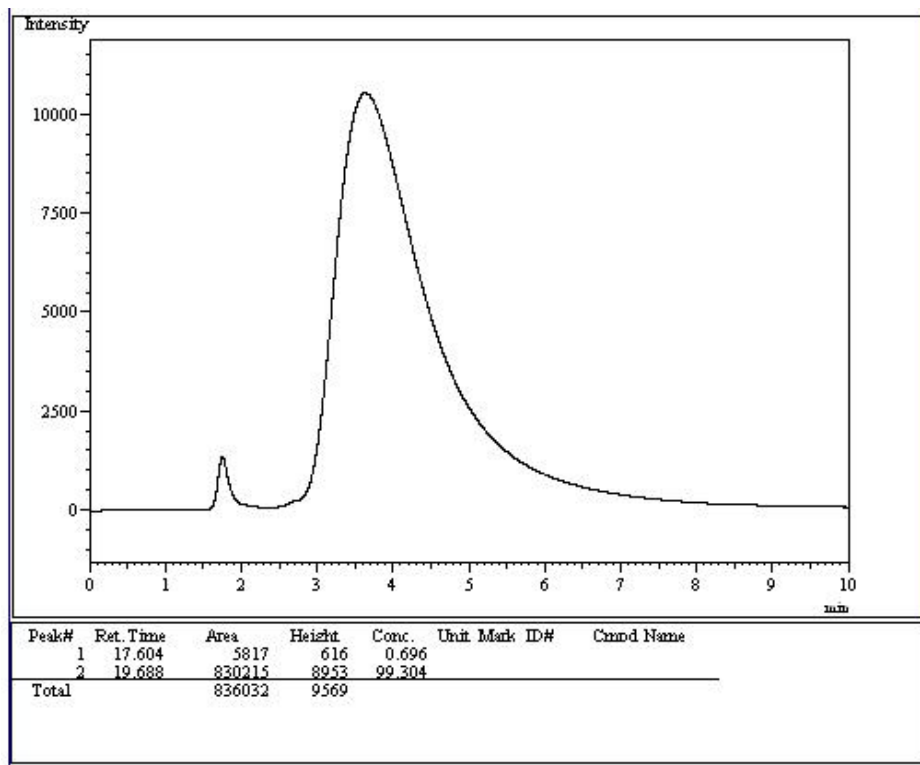


Fig. S14. IR spectrum of carbocation salt(s) resulting from the reaction of $\text{H}(\text{CHB}_{11}\text{F}_{11})$ with *n*-hexane. The spectrum of remnant unreacted acid has been subtracted.

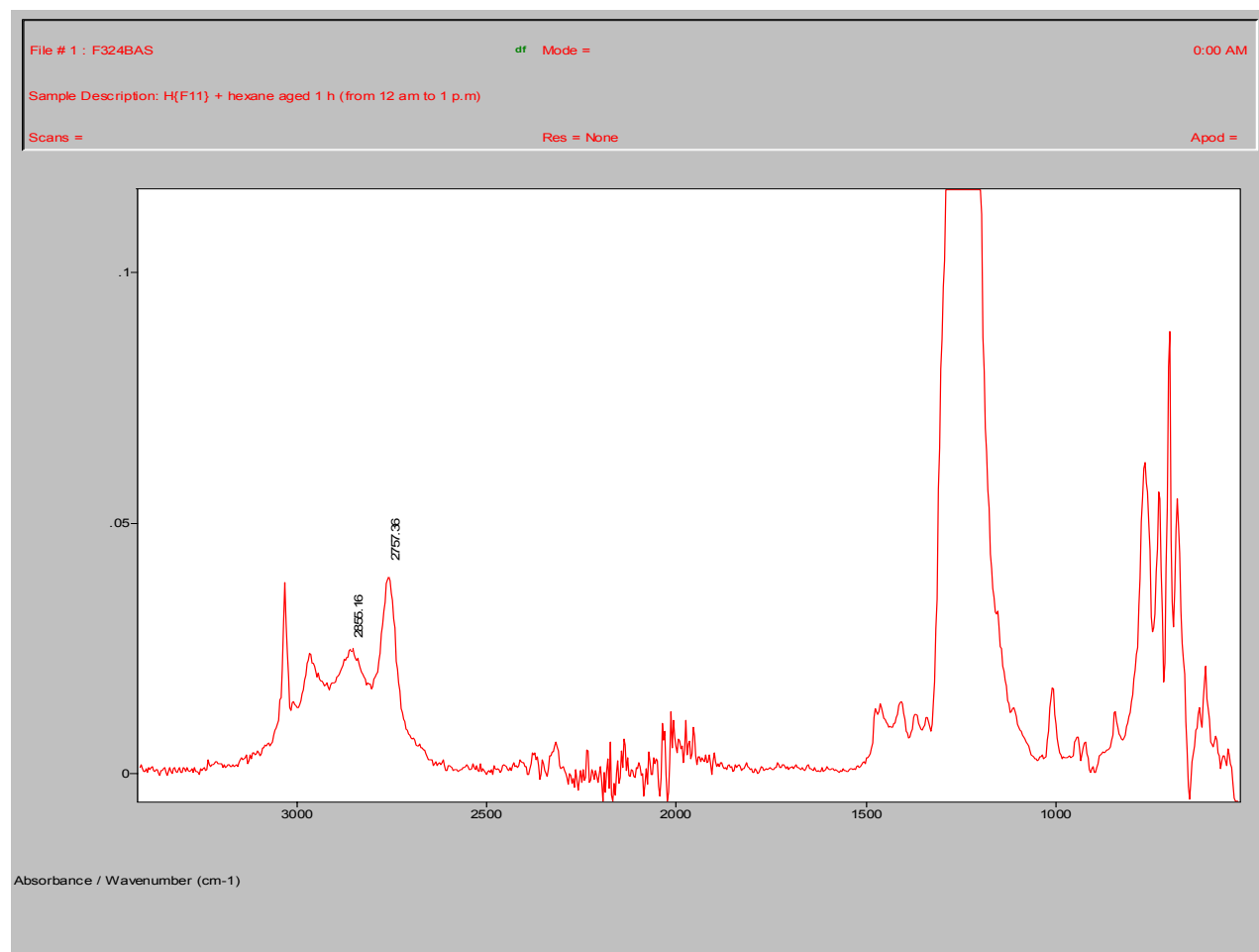


Fig. S15. IR spectrum of the *t*-butyl cation salt resulting from the reaction of H(CHB₁₁F₁₁) with *n*-butane. The spectrum of a small amount of unreacted acid has been subtracted.

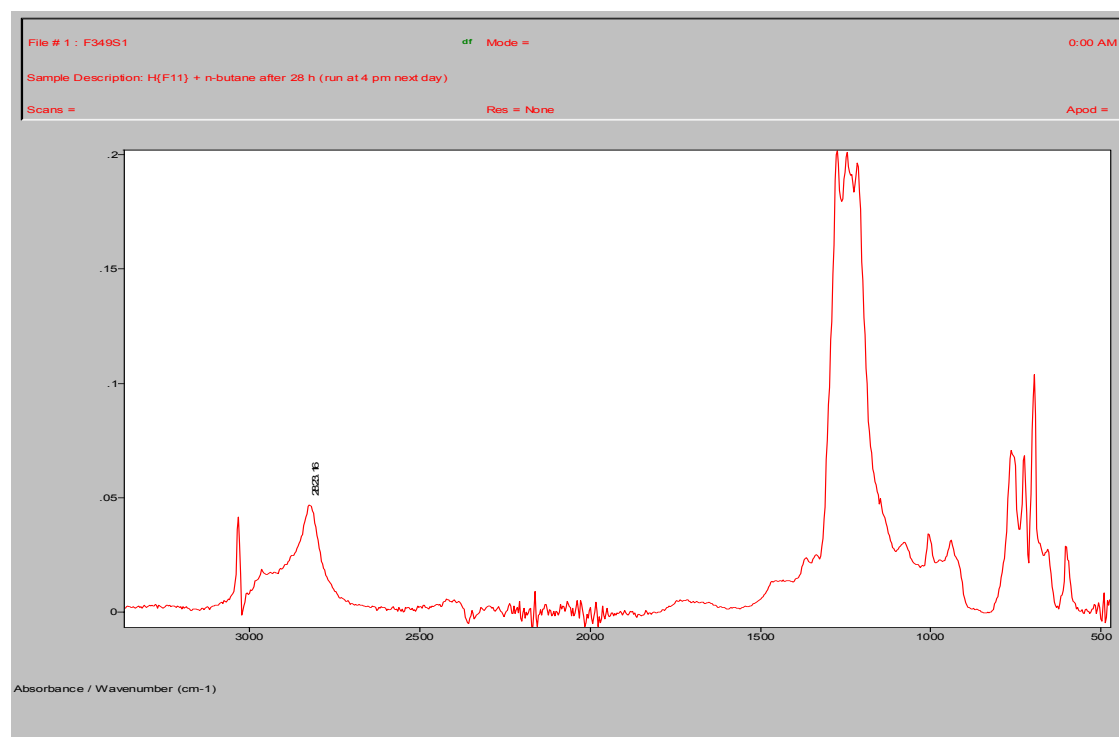


Fig. S16. IR spectrum of known [*t*-Bu⁺][CHB₁₁Cl₁₁⁻] for comparison to Fig. S15 above. Note the similarity in the shape of the broad νCH band near 2800 cm⁻¹. Attempts to subtract the respective anions from S15 and S16 only partially helps to reveal the identity of the cation because (a) the cation spectra are not expected to be identical -- due to differences in CH hydrogen bonding with basicity of anion, and (b) cation-anion interactions in the solid state change the *anion* spectra as well, so finding the correct anion spectrum to subtract is problematic. Nevertheless, see Fig. S17 on following page.

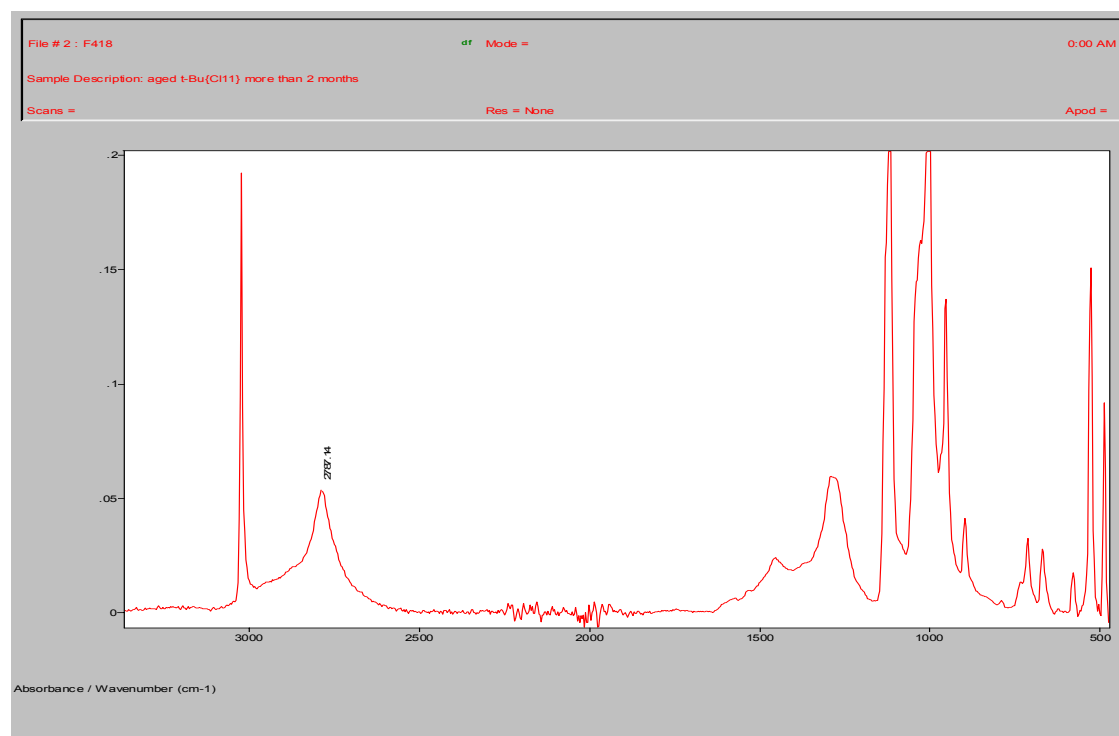


Fig. S17. Comparison of Figs. S15 (red) and S16 (black) showing coincidence of the two broad bands in the 1280-1400 cm^{-1} region arising from δCH of $t\text{-Bu}^+$ and inexact subtraction of the anion below 1400 cm^{-1} (using the anion spectrum of $[\text{Et}_2\text{Cl}][\text{CHB}_{11}\text{Cl}_{11}]$).

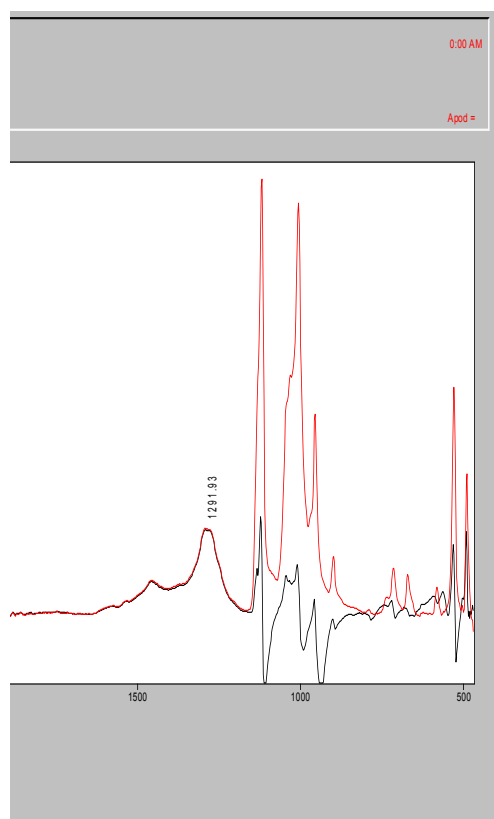


Fig. S18. Gas chromatographic trace of evolved hydrocarbon (hexene) from the reaction of C_6 carbocation $CHB_{11}F_{11}^-$ salt with NaH in $SO_2(l)$. Retention time (compound): 1.82 (Ar), 1.90 (SO_2), 3.62 (reference compound), 4.38 (hexene). The sample was prepared by dissolving NaH (excess) and the C_6 carbocation $CHB_{11}F_{11}^-$ salt in dry liquid SO_2 and stirring overnight at room temperature. After cooling to ca. $-5^\circ C$, SO_2 was allowed to boil off for several seconds and then, after warming the vessel to ca. $30^\circ C$, a $30\ \mu L$ sample of the remaining head gas was taken by syringe for gc/ms measurement.

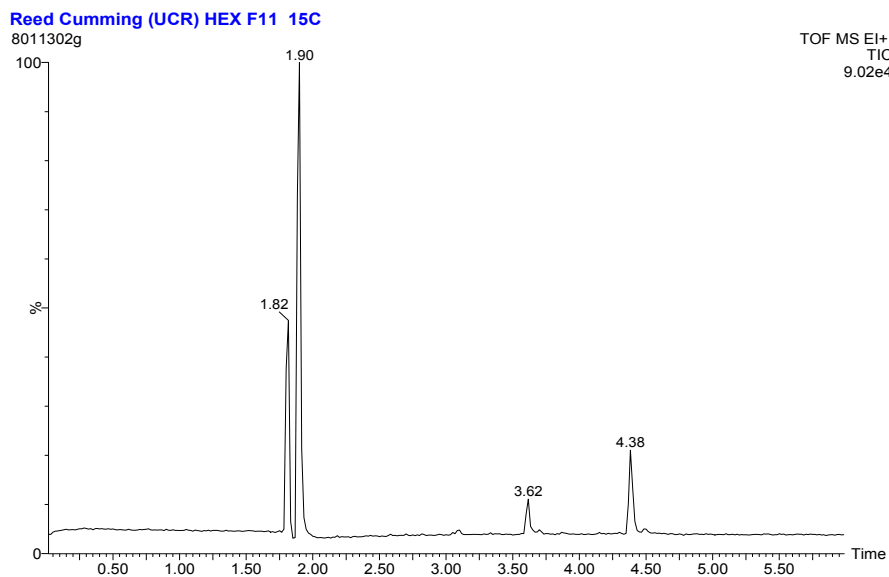


Fig. S19. Time of flight electron impact mass spectrum of hexene arising from deprotonation of C_6 carbocation $CHB_{11}F_{11}^-$ salt with NaH in liquid SO_2 .

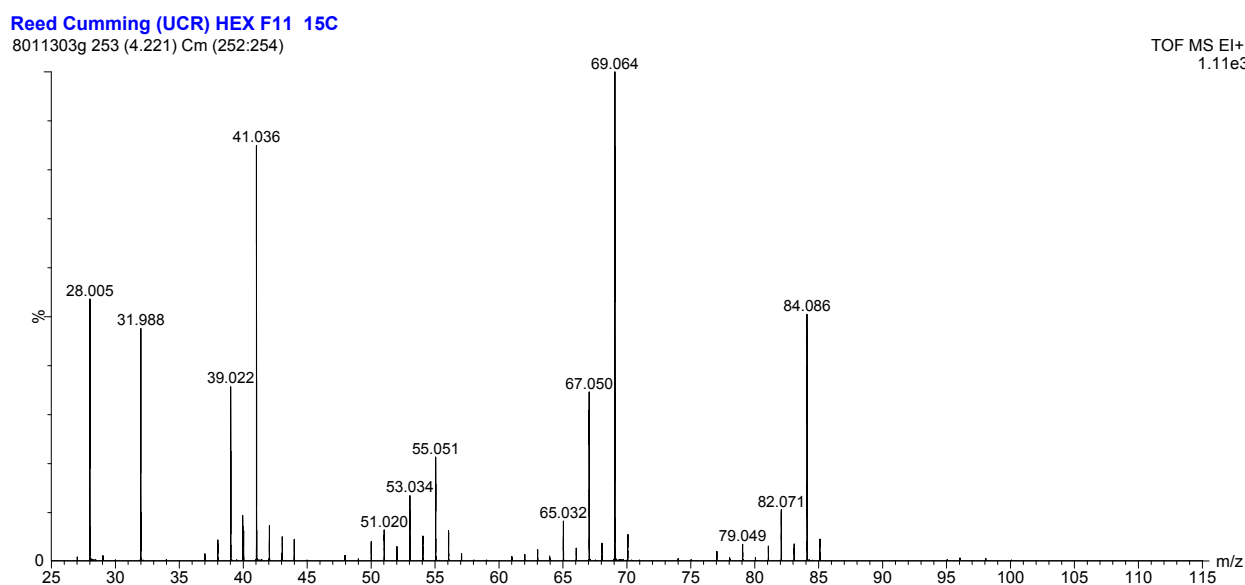


Fig. S20. Published electron impact mass spectra of various C_6 alkenes (as well as methyl-*cyclo*-pentane) with formula C_6H_{12} for comparison to Fig. S19.

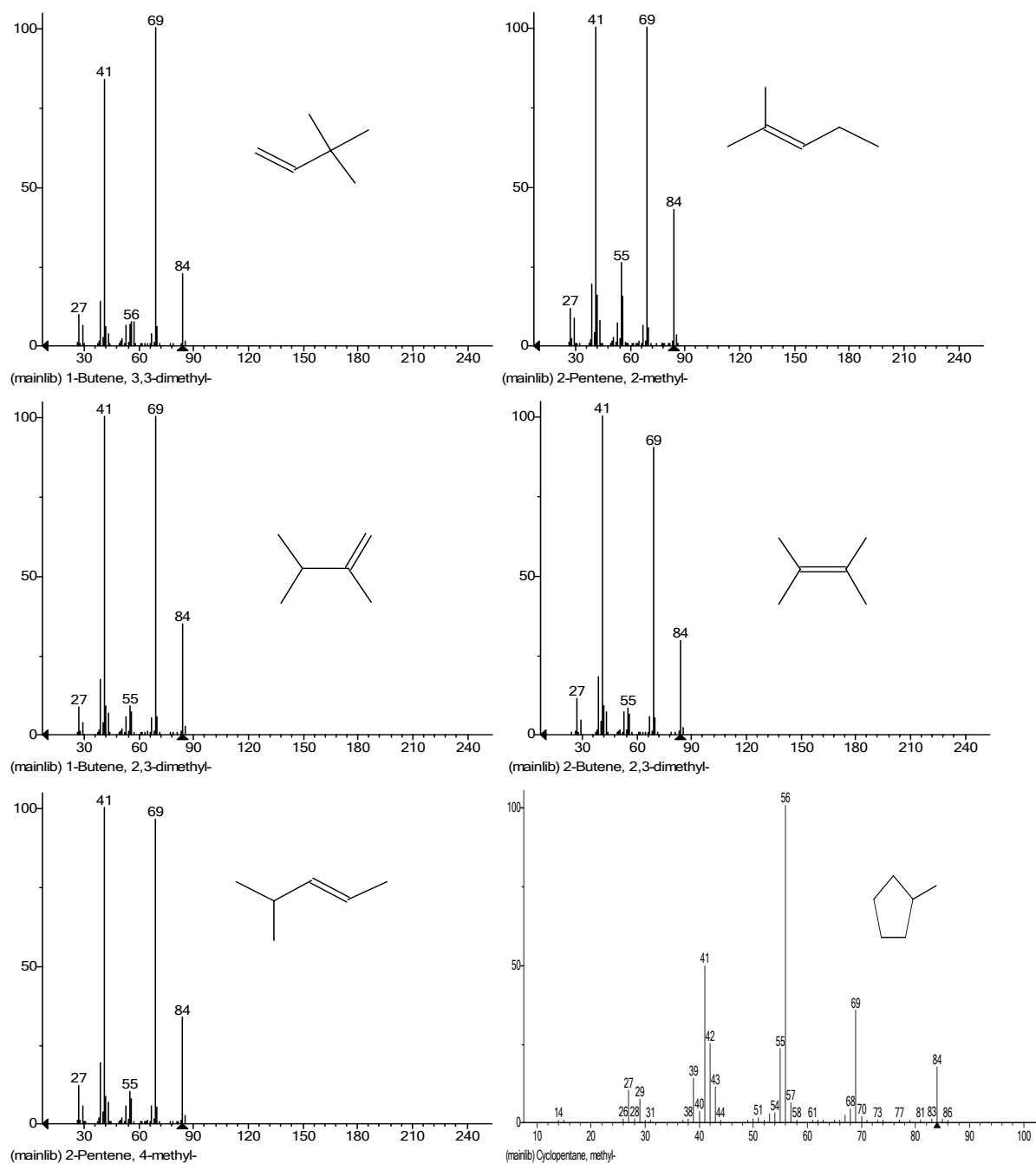


Fig. S21. Gas chromatograph of vapors above an intimately ground mixture of $\text{NaH}_{(s)}$ and C_6 carbocation salt isolated from the reaction of $\text{H}(\text{CHB}_{11}\text{F}_{11})$ with *n*-hexane. Retention time (compound): 1.80 (CO_2), 1.92 (*iso*-butane), 2.17 ref. compd., 2.23 (C_5H_{12} hydrocarbon), 2.28 ref. compd., 2.42 ref. compd., 2.67 (2,2-dimethylbutane), 2.80 ref. compd., 2.97 (2,3-dimethylbutane), 3.07 (2-methylpentane); 3.28 (3-methylpentane).

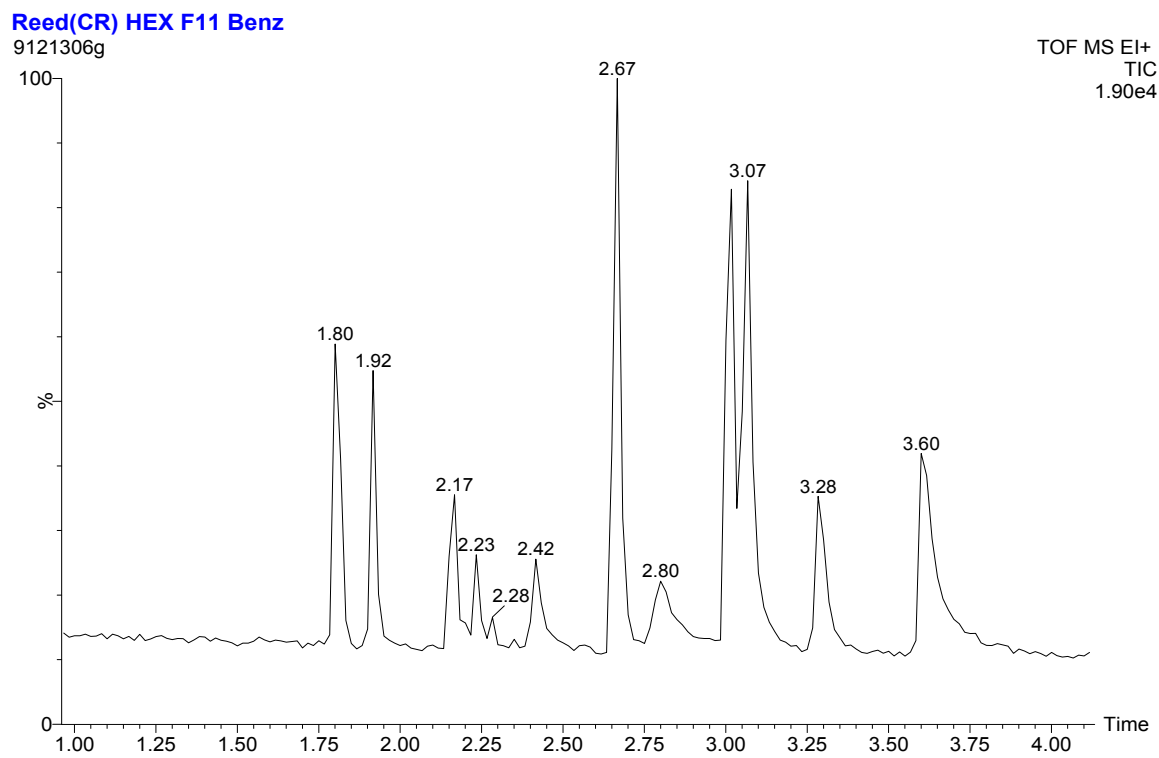


Fig. S22. Gas chromatogram of the head space vapors above an intimately ground mixture of $\text{NaH}_{(s)}$ and $t\text{-Bu}^+[\text{CHB}_{11}\text{F}_{11}]_{(s)}^-$ obtained from protonation of *n*-butane with $\text{H}(\text{CHB}_{11}\text{F}_{11})$ showing *iso*-butane as the major product (1.92). Retention time (compound): 1.82 (CO_2), 1.92 (*iso*-butane), 2.17, 2.42, 2.80 (reference compounds). Minor peaks at 2.05 and 2.25 correspond to traces of *n*-butane and a C_5H_{12} hydrocarbon, respectively, whose origin is uncertain.

